



## Authigenic pyrite framboids in sedimentary facies of the Mount Wawel Formation (Eocene), King George Island, West Antarctica

Anna MOZER

*Instytut Nauk Geologicznych PAN, Ośrodek Badawczy w Warszawie,  
Twarda 51/55, 00-818 Warszawa, Poland;*

*Zakład Biologii Antarktyki PAN, Ustrzycka 10/12, 02-141 Warszawa, Poland  
<amozer@twarda.pan.pl>*

**Abstract:** Pyrite framboids occur in loose blocks of plant-bearing clastic rocks related to volcano-sedimentary succession of the Mount Wawel Formation (Eocene) in the Dragon and Wanda glaciers area at Admiralty Bay, King George Island, West Antarctica. They were investigated by means of optical and scanning electron microscopy, energy-dispersive spectroscopy, X-ray diffraction, and isotopic analysis of pyritic sulphur. The results suggest that the pyrite formed as a result of production of hydrogen sulphide by sulphate reducing bacteria in near surface sedimentary environments. Strongly negative  $\delta^{34}\text{S}_{\text{VCDT}}$  values of pyrite (-30 – -25 ‰) support its bacterial origin. Perfect shapes of framboids resulted from their growth in the open pore space of clastic sediments. The abundance of framboids at certain sedimentary levels and the lack or negligible content of euhedral pyrite suggest pulses of high supersaturation with respect to iron monosulphides. The dominance of framboids of small sizes (8–16  $\mu\text{m}$ ) and their homogeneous distribution at these levels point to recurrent development of a laterally continuous anoxic sulphidic zone below the sediment surface. Sedimentary environments of the Mount Wawel Formation developed on islands of the young magmatic arc in the northern Antarctic Peninsula region. They embraced stagnant and flowing water masses and swamps located in valleys, depressions, and coastal areas that were covered by dense vegetation. Extensive deposition and diagenesis of plant detritus in these environments promoted anoxic conditions in the sediments, and a supply of marine and/or volcanogenic sulphate enabled its bacterial reduction, precipitation of iron monosulphides, and their transformation to pyrite framboids.

**Key words:** Antarctica, King George Island, Eocene, framboidal pyrite, bacterial sulphate reduction, sulphur isotopes.

### Introduction

One of the most common forms of pyrite in sedimentary rocks are framboids. Framboids, as defined by Ohfuji and Rickard (2005), are microscopic spheroidal

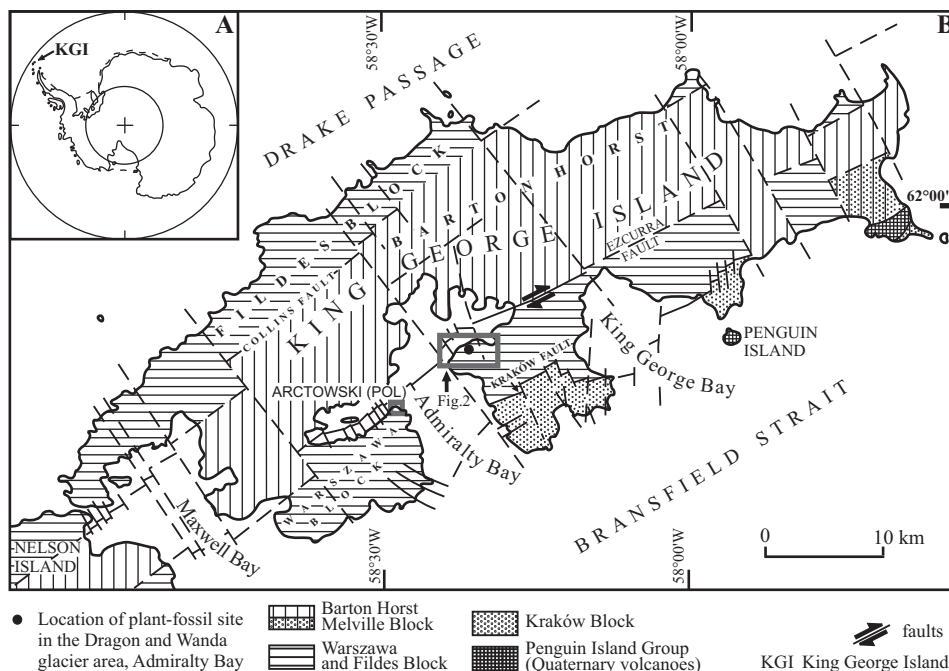


Fig. 1. A. Location of King George Island in Antarctica. B. Tectonic map of King George Island showing position of the Warszawa Block and location of plant fossil site in the Mount Wawel Formation. Map after Birkenmajer (1983).

to sub-spheroidal clusters of equidimensional and equimorphic microcrystals. This definition embraces three fundamental characteristics of framboids: (1) they are spheroidal to sub-spheroidal in form, (2) they are composed of densely packed discrete microcrystals, and (3) the microcrystals are equidimensional and equimorphic. Framboids in sedimentary facies originate due to crystallization of pyrite from amorphous or poorly ordered iron sulphides that precipitate in the form of spherical microbodies in the anoxic sulphidic environment (Berner 1970, 1984, 1985; Canfield 1989). These microspheres reflect precipitation from highly supersaturated fluids developed due to metabolic activity of sulphate reducing bacteria (Chambers and Trudinger 1979; Habicht and Canfield 1997; Wilkin and Barnes 1997a, b).

This paper presents pyrite framboids occurring in a plant-bearing volcano-sedimentary succession of the Mount Wawel Formation (Eocene) that crops out in the Dragon and Wanda glaciers area at Admiralty Bay, King George Island, West Antarctica (Fig. 1). Geochemical, textural, and morphological data are presented to support bacterial origin of the framboids during authigenesis of organic-rich sediments in terrestrial environments of the northern Antarctic Peninsula region.

## Geological background

King George Island (KGI) is located in the South Shetland Islands (Fig. 1) that make an outer magmatic arc related to the subduction-related magmatism in the northern Antarctic Peninsula region (Birkenmajer 1983, 2001). On the north it borders the South Shetlands subduction trench, which is a part of the Drake Passage tectonic structure. On the south it is separated from the crustal terrane of Antarctic Peninsula by a young rift and basin of the Bransfield Strait. KGI consists of several tectonic blocks showing considerable differences in stratigraphic succession, geological ages and character of rocks (Birkenmajer *et al.* 1991). The Warszawa Block occurs in the southern part of the island, and is dominated by volcanic and volcano-sedimentary formations of Paleogene age that are classified into the Admiralty Bay, Ezcurra Inlet, and Point Hennequin groups (Birkenmajer 2003).

The Mount Wawel Formation (300 m thick) constitutes the upper part of the Point Hennequin Group that crops out along Martel Inlet on the eastern side of Admiralty Bay (Fig. 2). The formation overlies the Viéville Glacier Formation, and its upper boundary is erosional (Birkenmajer 1980). It consists of several thick andesite lava flows, and embraces three informal sedimentary units containing plant remains: the Dragon Glacier plant beds, the Wanda Glacier plant beds, and the Mount Wawel plant beds (Birkenmajer 1981; Zastawniak *et al.* 1985; Zastawniak 1998). Abundant plant fossils, cases of caddisflies and associated trace fossils (Uchman *et al.* 2008) occur in clastic rocks distributed mainly in the form of loose blocks on lateral and marginal moraines of the Dragon and Wanda glaciers. A Middle Eocene to Late Oligocene age for the Point Hennequin Group was suggested on the basis of radiometric datings (Pankhurst and Smellie 1983; Smellie *et al.* 1984; Birkenmajer 1989, 2003). However, a new series of K-Ar datings of the

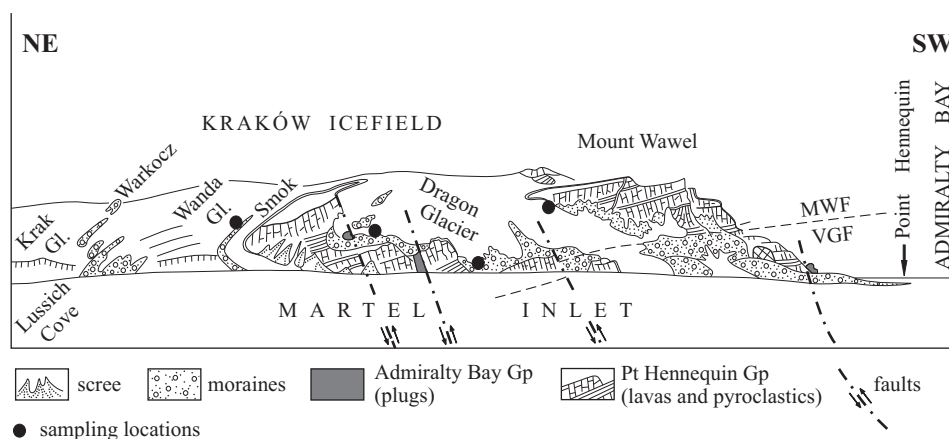


Fig. 2. Geological panorama of the southern coast of Martel Inlet in Admiralty Bay (after Birkenmajer 1983) showing location of samples analyzed in this paper.

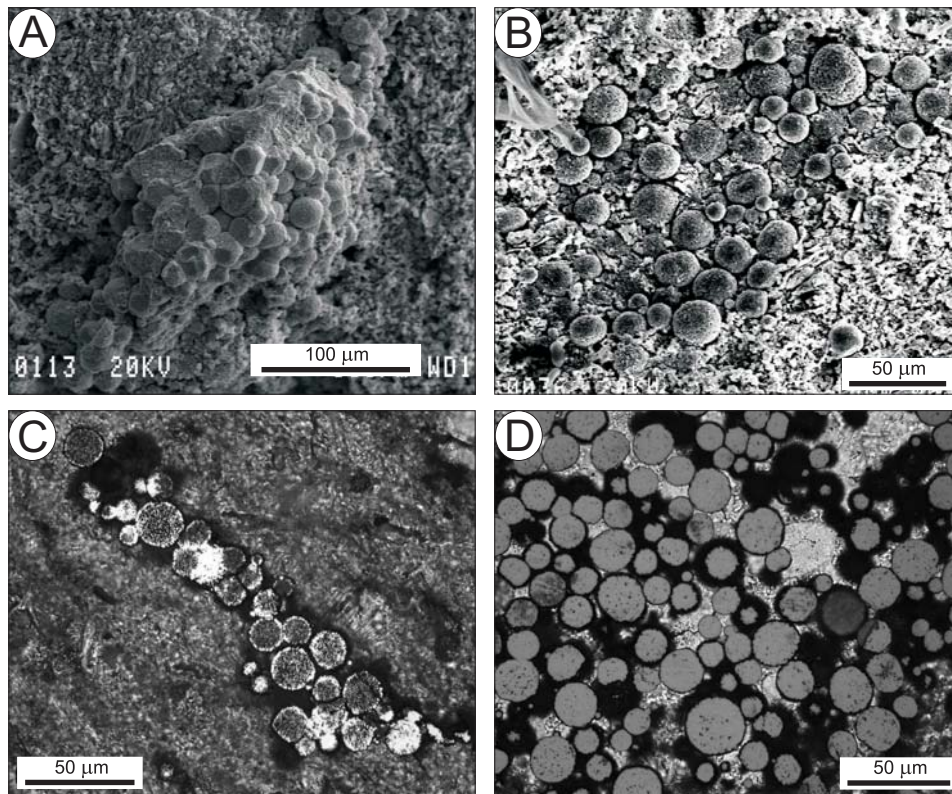


Fig. 3. Framboidal pyrite in sedimentary facies of the Mount Wawel Formation (I). **A, B.** SEM images of polyframboidal aggregates. **C, D.** TLM and RLM images of polyframboidal aggregates (normal light). Frambooids occurring in a mouldic pore after partial decomposition of a plant debris are shown in C.

Mount Wawel Formation points to its exclusive Eocene age (Z. Pécskay, personal communication). Loose blocks of plant-bearing clastic rocks in the Dragon and Wanda moraines have not been as yet precisely dated (Birkenmajer 1980, 1981, 1989; Zastawniak 1981; Zastawniak *et al.* 1985; Birkenmajer and Zastawniak 1989). Similar plant beds found in the Fildes Formation on Fildes Peninsula (Li 1994; Zhou 1994) and in the Point Thomas Formation in Ezcurra Inlet (KGI) have been dated as Eocene (Poole *et al.* 2001; Hunt and Poole 2003; Tatur *et al.* 2009).

Plant remains and the associated authigenic pyrite occur in fine-grained rocks, mostly in grey and greyish-brown mudstone, siltstone and claystone, which contain small-sized volcanic bombs (up to a few centimetres in size) and scattered finer volcanogenic clasts. The clastic material is dominated by recrystallized brown and green volcanic glass. The sediment reveals stratification emphasized by vertical changes in the grain size as well as by horizontal alignment of plant remains in fine-grained intervals. Sedimentary structures suggest deposition in stagnant and flowing water environments, with recurrent pulses of increased supply of plant ma-

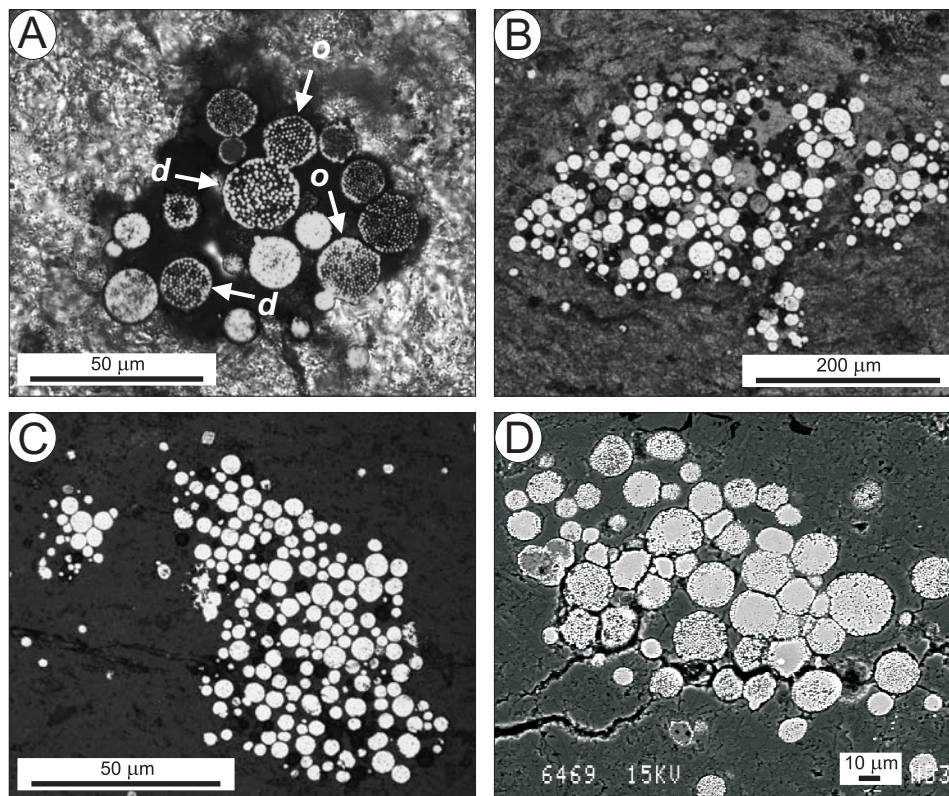


Fig. 4. Framboidal pyrite in sedimentary facies of the Mount Wawel Formation (II). A–C. TLM and RLM images of polyframboidal aggregates (normal light). Ordered (*o*) and disordered (*d*) framboids are shown in A. D. BSE image of polyframboidal aggregate.

terial. This material is represented by fragments of Gymnosperm shoots and Angiosperm leaves, various seeds and fruit scales as well as undefined plant detritus (Zastawniak *et al.* 1985). The Angiosperms are dominated by the genus *Nothofagus*, and the Gymnosperms by Podocarpaceae. This plant community resembles evergreen or deciduous forests, similar to the ones in the present-day Patagonia, New Zealand (Zastawniak 1981; Zastawniak *et al.* 1985; Birkenmajer and Zastawniak 1989), and south-east Australia (Zastawniak 1981). The forests covered slopes and valleys of mountainous landscape in the magmatic arc, providing plant material to the fresh-water and nearshore sedimentary environments (Poole *et al.* 2001; Hunt and Poole 2003).

## Materials and methods

The material analyzed in this paper was collected at three locations along the outcrop belt of the Mount Wawel Formation: (1) the lateral and marginal moraines

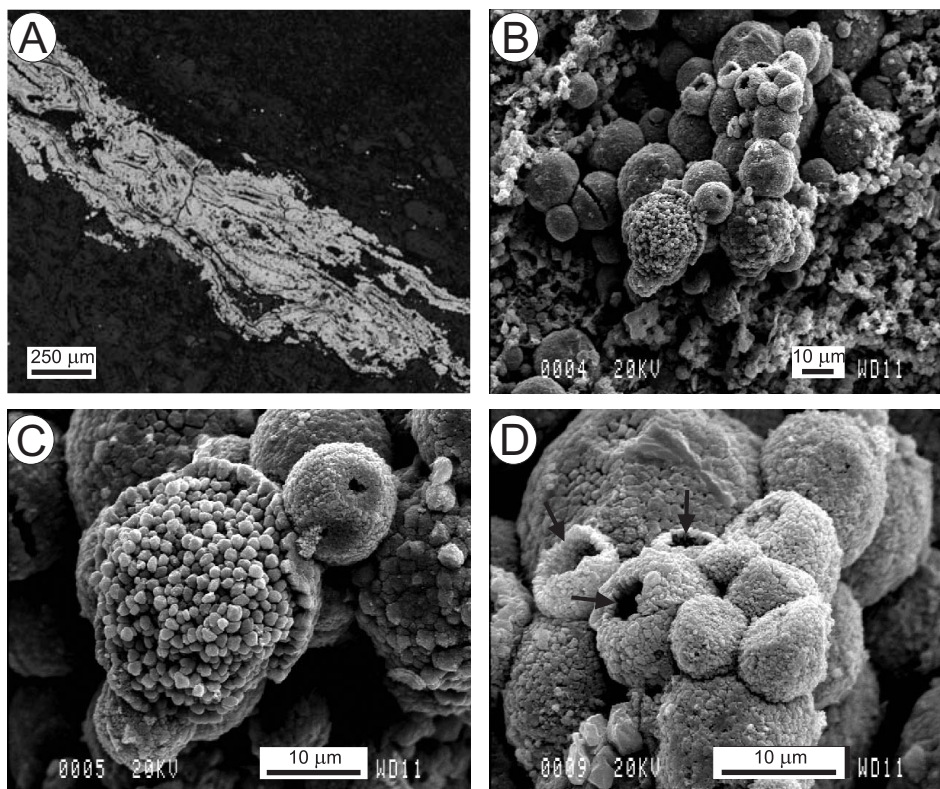


Fig. 5. Pyritic structures associated with framboids in sedimentary facies of the Mount Wawel Formation. A. Pyritized plant debris in a plant-bearing horizon. TLM and RLM image, normal light. B–D. Pyritic microcapsules showing empty interiors and apertures (*arrows*) open towards the pore space. SEM images.

of the Wanda Glacier, (2) the lateral moraines of the Dragon Glacier, and (3) the marginal moraines of the Dragon Glacier (Fig. 2). At these locations, large accumulations of loose blocks up to a few metres in size contain horizons and layers enriched in plant detritus and authigenic pyrite.

Pyrite was identified on the basis of petrographic observations under transmitted and reflected light microscopy (TLM and RLM), and scanning electron microscopy (SEM). The three-dimensional morphology of pyrite was studied on broken rock surfaces that were subjected to etching using hydrofluoric acid. After petrographic analysis in transmitted and reflected light, thin sections were coated with carbon and analyzed under SEM. A JEOL JXA 840A scanning electron microscope operating at a 15 kV accelerating voltage was used. Quantitative EDS analyses of pyrite were obtained using the same microscope, equipped with a THERMO NORAN VANTAGE EDS system. Operating conditions were a 15 kV acceleration voltage, 1 to 5 mm beam diameter, and 100 s counting time. Detection limits of the analyzed elements (S, Fe, Co, Ni, Cu, Zn) were better than 0.05 wt. %.

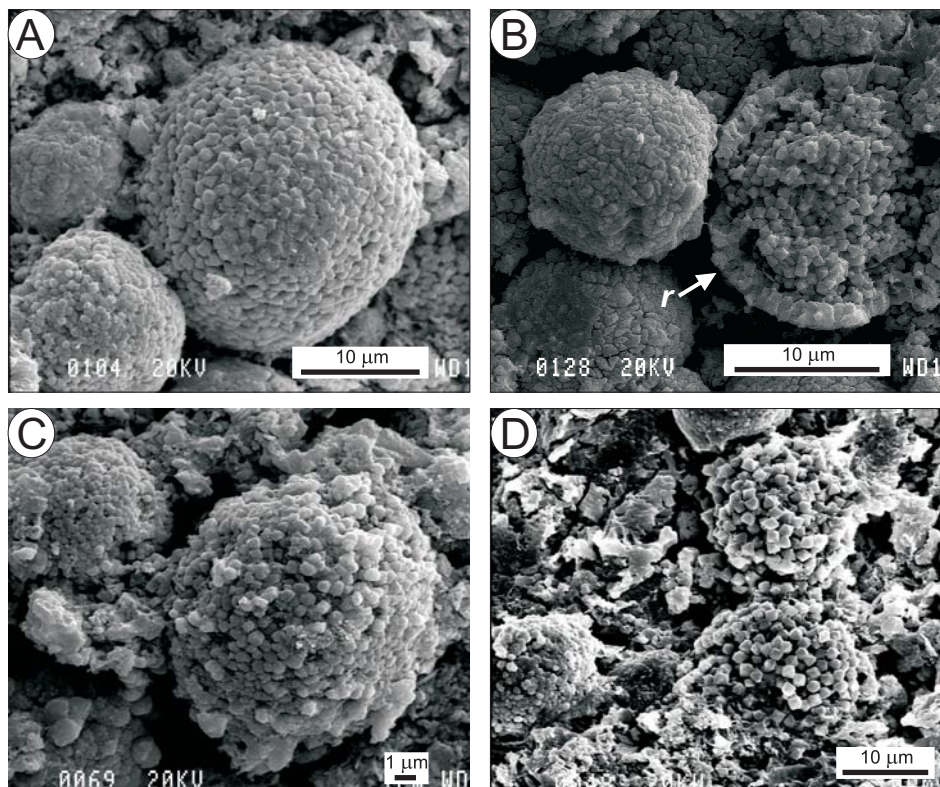


Fig. 6. Details of pyritic framboids in sedimentary facies of the Mount Wawel Formation (I). **A**. Example of ordered structure. **B–D**. Examples of disordered structure. A rim of elongated pyrite crystals (*r*) coating disordered framboid is shown in **B**. A–D SEM images.

Back-scattered electron images (BSE) were used to precisely locate analytical points on thin sections.

For the X-ray diffraction (XRD) and sulphur isotope (SI) analyses, the rock samples were crushed and powdered to the fraction 5–10 µm. Twenty and three samples containing framboidal pyrite have been selected for XRD and SI analyses, respectively. X-ray diffraction patterns were recorded on a SIGMA 2070 diffractometer using a curved position sensitive detector in the range 2–120° 2θ with CoKα radiation and 20 hour analysis time. DIFFRACTIONEL software v. 03/93 was used to process the obtained data. Isotopic composition of pyritic sulphur was analyzed in 1 to 5 g of sample. The sulphur extraction procedure was based on the method presented in Kolthoff and Sandell (1952), Canfield *et al.* (1986), Tuttle *et al.* (1986), and Bates *et al.* (1993). The samples were treated by reaction with a 1.0 M solution of chromium chloride (CrCl<sub>2</sub>) and 12 N HCl in proportion 2:1. Then the mixtures were boiled under an Ar flow. This procedure converted pyrite (FeS<sub>2</sub>) to hydrogen sulphide (H<sub>2</sub>S). A flow of Ar carried H<sub>2</sub>S through the apparatus, first through the buffer solution of 80% 1 M CH<sub>3</sub>COOH + 20% 1 M CH<sub>3</sub>COON at pH4

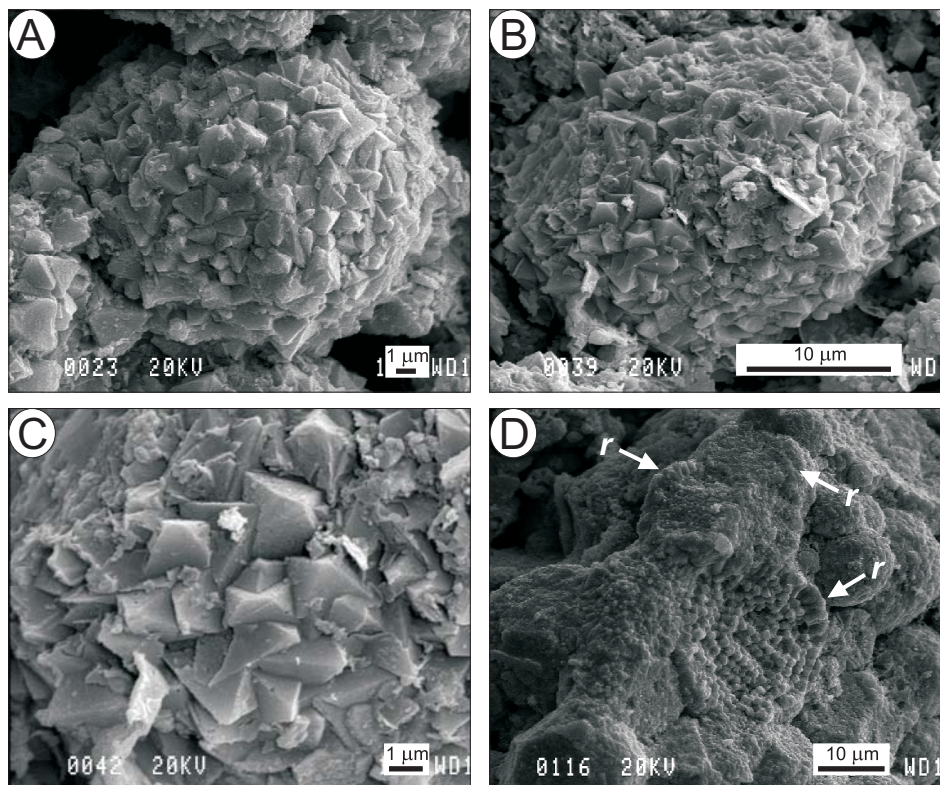


Fig. 7. Details of pyritic framboids in sedimentary facies of the Mount Wawel Formation (II). A–C. Framboids showing interlocking mosaic of recrystallized (cubic and/or octahedral) pyrite microcrystals. D. Pyrite rims (*r*) coating ordered framboids. A–D SEM images.

to remove chlorine compounds, and then to a vessel where  $H_2S$  reacted with  $AgNO_3$  to form  $Ag_2S$ .  $Ag_2S$  was collected by filtration, dried, and weighed. It was isotopically analyzed using a MAT 253 spectrometer equipped with a FLASH EA device in continuous flow mode. Sulphur isotope ratios are reported as  $\delta^{34}S$  notations relative to the Vienna Cañon Diablo Troilite standard (VCDT).

All samples analyzed in this paper are housed at the Institute of Geological Sciences, Polish Academy of Sciences in Warszawa.

## Results

In clastic rocks of the Mount Wawel Formation, pyrite occurs predominantly in the form of framboids that concentrate at discrete horizons enriched in plant detritus (Figs 3, 4). The framboids are found to have developed in open pore space, where they form polyframboidal seams and lenses up to a few mm in length. These pyritic bodies occur close to pyritized plant fragments, the latter showing pre-

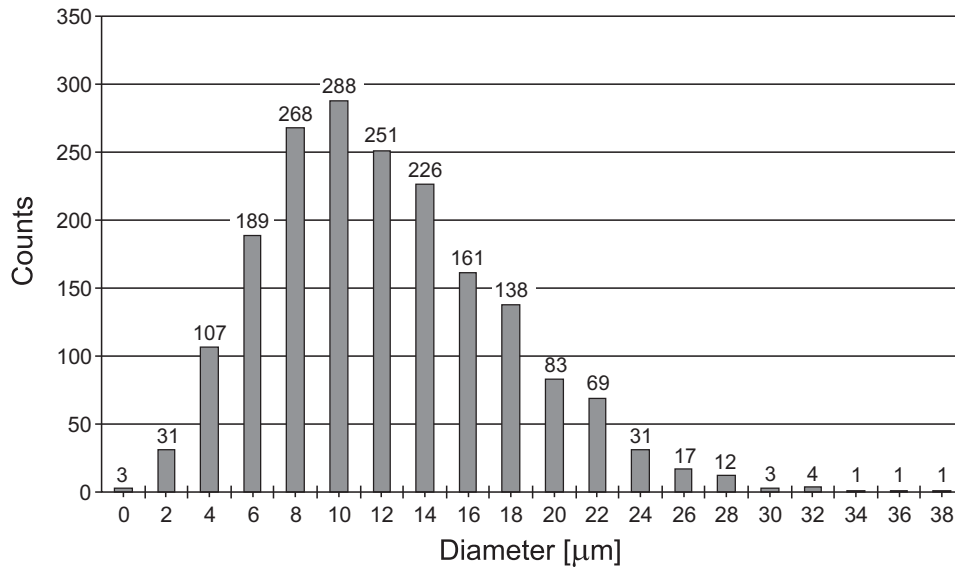


Fig. 8. Histogram showing the frequency of framboid diameter in sedimentary facies of the Mount Wawel Formation.

Table 1  
Molar composition of sulphur and iron in framboidal pyrite. Location of analytical points is shown in Fig. 11.

No. of analysis	Pyritic S (mol %)	Pyritic Fe (mol %)
1	64.73	34.34
2	64.78	34.60
3	64.41	35.01
4	64.43	34.32
5	65.19	34.58
6	65.05	34.83
7	64.82	34.90
8	64.83	34.49
9	64.02	35.29
10	64.46	35.22
11	64.06	35.57
12	62.80	36.71
13	65.21	34.68
14	65.56	34.14
15	63.62	35.60
Min. value	62.80	34.14
Max. value	65.56	36.71
Average	64.53	34.95

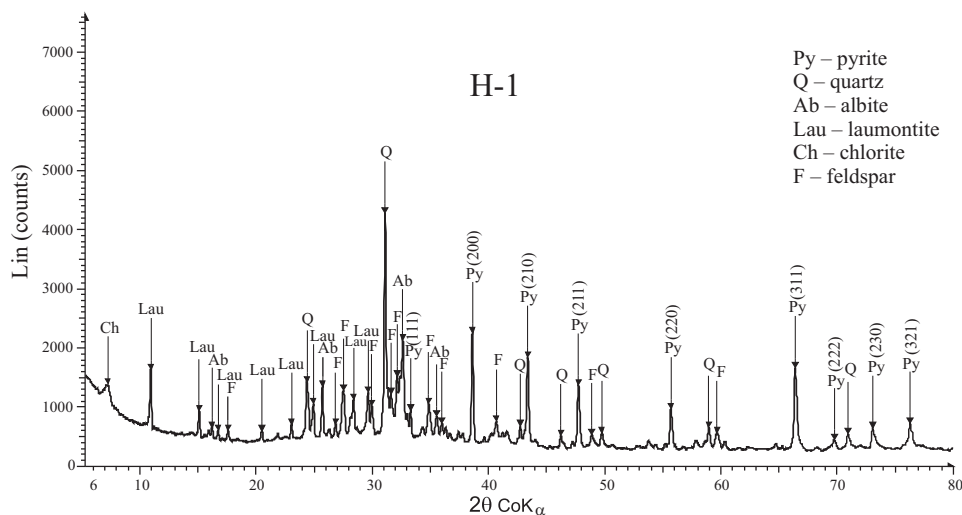


Fig. 9. X-ray diffraction (XRD) pattern of plant-bearing mudstone enriched in framboidal pyrite. Numbers in brackets indicate  $hkl$  reflections of pyrite. Dragon Glacier marginal moraine; sample H-1.

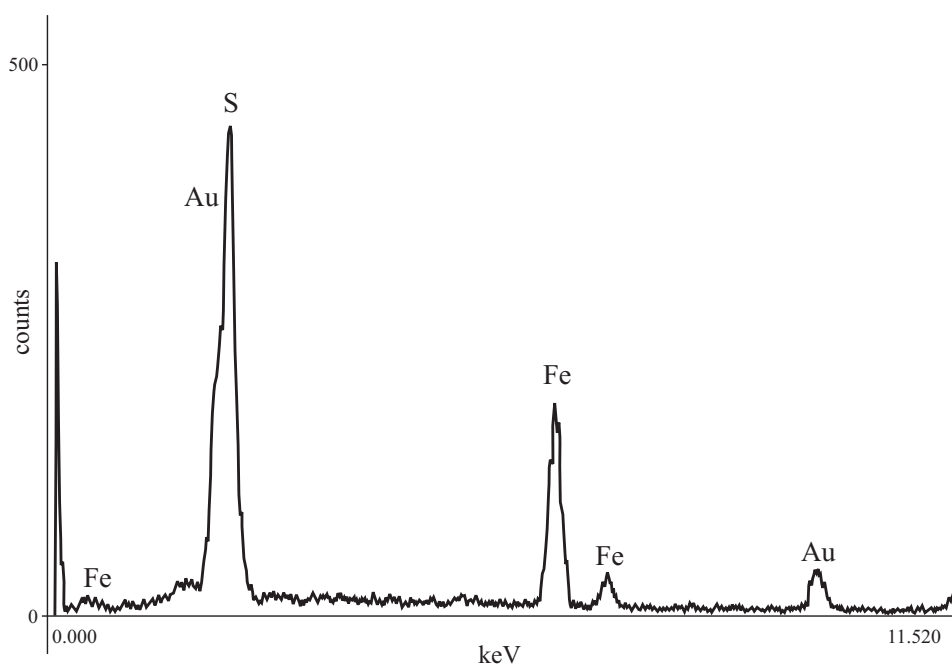


Fig. 10. EDS spectrum of a pyrite framboid. Wanda Glacier marginal moraine; sample S-2.

served anatomic details without any compactional deformation (Fig. 5A). Associated with pyrite framboids occur pyritic microcapsules (8–12  $\mu\text{m}$ ), often showing empty interiors and apertures open towards the pore space (Fig. 5B–D).

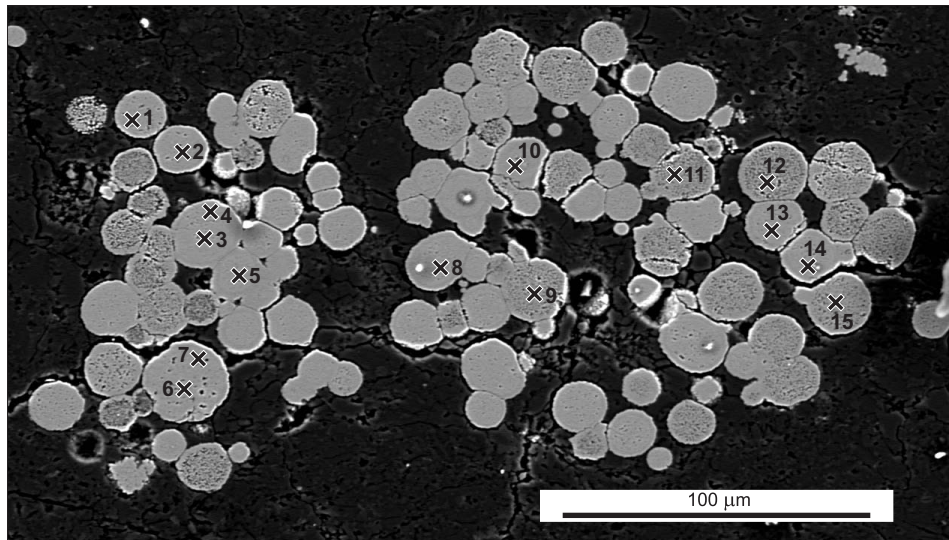


Fig. 11. BSE image of polyframboidal pyrite showing location of EDS point analyses listed in Table 1. Dragon Glacier marginal moraine; sample S-2.

The framboids are spheroidal to sub-spheroidal in form; however, some framboids reveal slightly ellipsoidal shapes (Figs 3D, 4A–D). They are composed of densely packed discrete microcrystals. The microcrystals reveal equidimensional and equimorphic structure. Based on SEM observations, two groups of the framboid structure can be discerned: ordered and disordered. The ordered structure consists of microcrystals that show almost uniform morphological alignments (Figs 4A, 6A), whereas the disordered structure is made up of chaotically distributed microcrystals (Figs 4A, 6B–D). The ordered forms are more frequently observed. Framboids showing overgrowths with layers of densely packed, elongated pyrite crystals are also observed (Figs 6B, 7D). Some framboids show diagenetic recrystallization that is manifested by replacements by larger cubic and/or octahedral crystals (Fig. 7A–C).

Statistical analysis of the framboid diameters measured in thin sections (more than 1,400 measurements) shows that the framboids vary in size from  $< 1 \mu\text{m}$  up to  $40 \mu\text{m}$ , with more than 50% falling in a range between  $8 \mu\text{m}$  and  $16 \mu\text{m}$  (Fig. 8). Large scattered framboids ( $30\text{--}40 \mu\text{m}$ ) were observed in all the investigated samples.

The results of XRD analysis show the presence of pyrite, without any detectable admixture of other sulphide minerals (Fig. 9). The results of EDS analysis show that most of the framboids are composed of pure pyrite, with the atomic Fe:S ratio close to 1:2 (Table 1, Figs 10, 11). Minor amounts of iron oxides have been detected in external parts of some framboids, possibly resulting from epigenetic oxidation of pyrite. In some framboids, trace amounts of Co, Ni, Cu, and Zn were detected.

The  $\delta^{34}\text{S}$  values of framboidal pyrite in three analyzed samples fall in a narrow range between  $-30\text{‰}$  and  $-25\text{‰}$  (Table 2).

Table 2  
Results of sulphur isotopic analysis ( $\delta^{34}\text{S}_{\text{VCDT}}\text{‰}$ ) of framboidal pyrite

Sample	$\delta^{34}\text{S}\text{ (‰)}$
H-1	-25.4
S-2	-29.2
F-2	-30.1

## Discussion

Sulphur may be present in sedimentary facies in the form of iron monosulphides (mackinawite, pyrrhotite or an amorphous phase), elemental sulphur, sulphates, organically-bound sulphur, and most commonly as pyrite (Canfield *et al.* 1986; Gorjan *et al.* 2003). The content and speciation of sulphur in sediment is related to the dominant type of diagenetic environment, in which various sulphur compounds are deposited as a result of its oxidation and/or reduction reactions (Berner 1974, 1984; Goldhaber and Kaplan 1974). Therefore, sulphur is considered a tracer of biogeochemical processes in sedimentary environments, and used as a proxy of paleoredox conditions in the geological record (*e.g.* Jones and Manning 1994; Lyons *et al.* 2003). The prevailing occurrence of authigenic pyrite is thought to reflect dominant anoxic sulphidic conditions (Raiswell *et al.* 1988). However, this pyrite can have diverse morphologies. Two of the most commonly observed are framboids and micron-sized euhedral (microgranular) crystals (Wang and Morse 1996; Taylor and Macquaker 2000). It has been argued that euhedral pyrite precipitates from porewaters oversaturated with respect to pyrite, but undersaturated with respect to iron monosulphides (Wang and Morse 1996). In contrast, pyrite framboids are commonly believed to have formed through iron monosulphide intermediates, from porewaters supersaturated with respect to both pyrite and iron monosulphides (Sweeney and Kaplan 1973; Morse *et al.* 1987; Roberts and Turner 1993; Taylor and Macquaker 2000).

In the study material, sulphur is predominantly bound in the form of pyrite framboids. The absence of euhedral pyrite indicates that the early phase of framboidal pyrite formation in sediments of the Mount Wawel Formation was associated with high supersaturation conditions with respect to iron monosulphides. Framboids are abundant throughout all the analyzed pyritization horizons and layers, where they are associated with pyritized detritus of higher plants showing well-preserved anatomic features. Results of experimental precipitation of pyrite within cells of higher plants at ambient temperatures were described in detail by Rickard *et al.* (2007). The presence of pyrite in that form is indicative of point concentration of ions participated in the chemical reaction ( $\text{HS}^-$  and  $\text{Fe}^{2+}$ ). High con-

centration of these ions leads to abrupt precipitation of iron monosulphides showing microglobular fabric. The abundance of well-developed framboids indicates that their formation was a relatively rapid process associated with the presence of highly reactive organic matter (Billon *et al.* 2007). The nature of the preserved plant detritus in sediments of the Mount Wawel Formation suggests pulses of enhanced deposition of fresh organic matter from the immediate neighbourhood, which is consistent with paleoenvironmental reconstructions of the plant-bearing strata (Zastawniak 1981; Zastawniak *et al.* 1985; Birkenmajer 1989; Poole *et al.* 2001; Hunt and Poole 2003).

Investigations of modern and ancient sedimentary environments suggest that the distribution of sizes of framboids is a reliable indicator of the extent of anoxic sulphidic conditions (Wilkin *et al.* 1996). Under euxinic conditions, syngenetic framboids form directly in the water column, reaching maximum diameter of approximately 5  $\mu\text{m}$  before falling out of the water column. They do not continue to grow after the accumulation in bottom sediments since they are no longer close to the redox boundary. In contrast, in sedimentary environments underlying dysoxic or oxic water column the framboids are larger and vary in size. As reported by Marynowski *et al.* (2007), a further increase of size may be caused only by diagenetic changes, such as formation of euhedral pyrite crystals. Wilkin *et al.* (1996), Wignall and Newton (1998), Wignall *et al.* (2010), Bond *et al.* (2010) suggest that larger framboids form within the sediments below an oxic and/or dysoxic water column. They observe that in sediments accumulated in euxinic environments the mean diameter of framboids is small (2.7–3.2  $\mu\text{m}$ ), and that framboids bigger than 10  $\mu\text{m}$  do not occur. The mean diameter increases under conditions of incipient dysoxia, and there may appear single framboids of more than 10  $\mu\text{m}$  in size. On the other hand, under strictly dysoxic conditions a rapid increase of framboid diameter is observed.

In all the samples investigated here, the framboids are characterized by a wide range of diameters from < 1  $\mu\text{m}$  up to 40  $\mu\text{m}$ , which confirms the development of anoxic sulphidic conditions within the sediment in well-aerated terrestrial environments. The abundance of framboids of small sizes (8–16  $\mu\text{m}$ ) in the plant-bearing horizons suggests that these conditions developed repeatedly, and led to rapid pulses of iron monosulphide precipitation associated with intense decomposition of organic matter. All the framboids are found to occur in the primary pore space without any traces of compressional deformation (*e.g.* flattening), which suggests that their pyritic structure have formed before any compaction of the sediment, *i.e.* very early during authigenesis. Incorporation of elemental sulphur originated either as a result of hydrogen sulphide oxidation or sulphate reduction was a likely scenario for transformation of monosulphides into pyrite (Berner 1970; Middelburg 1991; Billon *et al.* 2007).

It is generally accepted that the formation of framboidal pyrite in sedimentary environments is closely associated with activity of sulphate reducing bacte-

ria. Bacterial sulphate reduction is a low temperature process; and it is common in diagenetic settings from 0°C up to about 60–80°C at maximum (Machel 2001; Canfield *et al.* 2006). Above this temperature range, almost all sulphate reducing bacteria cease to metabolize. Pyritic horizons observed in the Mount Wawel Formation represent recurrent events of rapid precipitation that followed deposition of plant detritus and intense decomposition of organic matter. Associated with the framboids occur pyritic microcapsules, which are interpreted to represent authigenic mineral encrustations on microbial cells showing metabolic activity (Krajewski *et al.* 1994). The pyritized microbial ultrastructures document an abundance of microbial communities in the sediment, and confirm the formation of pyrite framboids at sedimentary temperatures. However, volcanic bombs found in some plant-bearing horizons suggest deposition in close proximity to volcanic activity.

It is well known that the isotopic composition of sulphur in sedimentary pyrite corresponds to the isotopic composition of the dissolved sulphide in the precipitating medium (Butler *et al.* 2004). During bacterial sulphate reduction, the light sulphur isotope ( $^{32}\text{S}$ ) is preferentially metabolized causing the generated hydrogen sulphide to be isotopically light compared to the source sulphate (Kaplan and Rittenberg 1963). Laboratory and field studies show that a common sulphur isotope fractionation during this process ranges between 20‰ and 40‰ (Butler *et al.* 2004; Mangalo *et al.* 2007). The  $\delta^{34}\text{S}$  values of pyrite in the Mount Wawel Formation fall in a narrow range from -30‰ to -25‰, suggesting that the source sulphate had isotopic composition roughly between 0‰ and +20‰. Sulphate in the Eocene sedimentary environments of KGI could originate either from volcanic eruptions or from sea spray, or represent a mixture of the two sources. The  $\delta^{34}\text{S}$  values for volcanic andesite-type rocks range from 0‰ to +20‰ (Torssander 1992; Marini *et al.* 2002; Mazot *et al.* 2007). The isotopic composition of sulphur in marine sulphate is close to +22‰ (Thode 1991), and similar values are expected to have dominated the Paleogene marine water (Ayora *et al.* 1995). It seems therefore likely that the sulphate subjected to bacterial reduction in sediments of the Mount Wawel Formation was of marine or mixed marine-volcanic origin.

## Conclusions

(1) The plant-bearing clastic facies of the Mount Wawel Formation (Eocene), King George Island, West Antarctica is enriched in authigenic pyrite, which occurs mostly in the form of framboids associated with pyritized plant debris.

(2) The pyrite framboids originated in the nearsurface environment of clastic sediments, where enhanced degradation of organic matter contributed to the development of anoxic sulphidic conditions. Isotopic composition of pyritic sulphur indicates that hydrogen sulphide generated in this environment was a result of activity of

sulphate reducing bacteria. Textural and chemical features of framboids suggest that their formation involved intermediate precipitates of amorphous or poorly ordered iron monosulphides, followed by crystallization of the mineral phase.

(3) The clastic facies of the Mount Wawel Formation records sedimentation in local depressions and coastal areas on a young magmatic island arc, with recurrent events of enhanced supply of plant detritus from forest-covered mountainous landscape. The abundance of authigenic pyrite in this facies suggests that there was a supply of marine or mixed marine-volcanic sulphate to sedimentary environments of the arc islands.

**Acknowledgements.** — This paper was supported by a research project of the Ministry of Science and Higher Education No. DWM/N8IPY/2008. I am grateful to K.P. Krajewski and to A. Tatur for providing me with analytical material for this study as well as for helpful discussions and comments. I also thank B. Łącka, P. Zawidzki and R. Orłowski for their help during laboratory work. The sulphur isotope analysis was done at the Stable Isotope Laboratory, Institute of Geological Sciences, Polish Academy of Sciences, in Warszawa. Special thanks are due to the reviewers K. Birkenmajer and D.P.G. Bond, whose comments have improved this paper.

## References

- AYORA C., TABERNER C., PIERRE C. and PUEYO J.J. 1995. Modeling the sulfur and oxygen isotopic composition of sulfates through a halite-potash sequence: Implications for the hydrological evolution of the Upper Eocene Southpyrenean basin. *Geochimica et Cosmochimica Acta* 59: 1799–1808.
- BATES A.L., SPIKER E.C., OREM W.H. and BURNETT W.C. 1993. Speciation and isotopic composition of sulfur in sediments from Jellyfish Lake, Palau. *Chemical Geology* 106: 63–76.
- BERNER R.A. 1970. Sedimentary pyrite formation. *American Journal of Science* 268: 1–23.
- BERNER R.A. 1974. Kinetic models for the early diagenesis of nitrogen, sulfur, phosphorus, and silicon in anoxic marine sediments. In: E.D. Goldberg (ed.) *The Sea* 5, Wiley, New York: 427–450.
- BERNER R.A. 1984. Sedimentary pyrite formation: An update. *Geochimica et Cosmochimica Acta* 48: 605–615.
- BERNER R.A. 1985. Sulphate reduction, organic matter decomposition and pyrite formation. *Philosophy Transactions Royal Society of London A* 315: 25–38.
- BILLON G., THOUMELIN G., BARTHE J.F. and FISHER J.C. 2007. Variations of fatty acids during the sulphidization process in the Authie Bay sediments. *Soil Sediments* 7: 17–24.
- BIRKENMAJER K. 1980. Tertiary volcanic-sedimentary succession at Admiralty Bay, King George Island (South Shetland Islands, Antarctica). *Studia Geologica Polonica* 64: 8–65.
- BIRKENMAJER K. 1981. Lithostratigraphy of the Point Hennequin Group (Miocene volcanics and sediments) at King George Island (South Shetland Islands, Antarctica). *Studia Geologica Polonica* 72: 59–73.
- BIRKENMAJER K. 1983. Late Cenozoic phases of block-faulting on King George Island (South Shetland Islands, Antarctica). *Bulletin, Académie Polonaise des Sciences: Terre*, 30: 21–32.
- BIRKENMAJER K. 1989. A guide to Tertiary geochronology of King George Island, West Antarctica. *Polish Polar Research* 10: 555–579.
- BIRKENMAJER K. 2001. Mesozoic and Cenozoic stratigraphic units in parts of the South Shetland Islands and Northern Antarctic Peninsula (as used by the Polish Antarctic Programmes). *Studia Geologica Polonica* 118: 5–188.

- BIRKENMAJER K. 2003. Admiralty Bay, King George Island (South Shetland Islands, West Antarctica): A geological monograph. *Studia Geologica Polonica* 120: 5–73.
- BIRKENMAJER K. and ZASTAWNIAK, E. 1989. Late Cretaceous–early Tertiary floras of King George Island, West Antarctica: their stratigraphic distribution and paleoclimatic significance. In: J.A. Crame (ed.) *Origins and Evolution of the Antarctic Biota. Geological Society Special Publications* 47: 227–240.
- BIRKENMAJER K., FRANCALANCI L. and PECCERILLO A. 1991. Petrological and geochemical constraints on the genesis of Mesozoic–Cenozoic magmatism of King George Island, South Shetland Islands, Antarctica. *Antarctic Science* 3: 293–308.
- BOND D.P.G. and WIGNALL P.B. 2010. Pyrite framboid study of marine Permian–Triassic boundary sections: A complex anoxic event and its relationship to contemporaneous mass extinction. *Geological Society of America Bulletin* 122: 1265–1279.
- BUTLER I.B., BÖTTCHER M.E., RICKARD D. and OLDROYD A. 2004. Sulfur isotope partitioning during experimental formation of pyrite via the polysulfide and hydrogen sulfide pathways: implications for the interpretation of sedimentary and hydrothermal pyrite isotope records. *Earth and Planetary Science Letters* 228: 495–509.
- CANFIELD D.E. 1989. Reactive iron in marine sediments. *Geochimica et Cosmochimica Acta* 53: 619–632.
- CANFIELD D.E., OLESEN C.A. and COX R.P. 2006. Temperature and its control of isotope fractionation by a sulfate-reducing bacterium. *Geochimica et Cosmochimica Acta* 70: 548–561.
- CANFIELD D.E., RAISWELL R., WESTRICH J.T., REAVES C.M. and BERNER R. 1986. The use of chromium reduction in the analysis of reduced inorganic sulfur in sediments and shales. *Chemical Geology* 54: 149–155.
- CHAMBERS L.A. and TRUDINGER P.A. 1979. Microbiological fractionation of stable sulfur isotopes: A review and critique. *Geomicrobiology Journal* 1: 249–293.
- GOLDHABER M.B. and KAPLAN I.R. 1974. The sulfur cycle. In: E.D. Goldberg (ed.) *The Sea* 5, Wiley, New York: 569–655.
- GORJAN P., WALTER M.R. and SWART R. 2003. Global Neoproterozoic (Sturtian) post-glacial sulfide-sulfur isotope anomaly recognized in Namibia. *Journal of African Earth Sciences* 36: 89–98.
- HABICHT K.S. and CANFIELD D.E. 1997. Sulphur isotope fractionation during bacterial sulphate reduction in organic-rich sediments. *Geochimica et Cosmochimica Acta* 61: 5351–5361.
- HUNT R.J. and POOLE I. 2003. Paleogene West Antarctic climate and vegetation history in light of new data from King George Island. In: S.L. Wing, P.D. Gingerich, B. Schmitz and E. Thomas (eds) *Causes and Consequences of Globally Warm Climates in the Early Paleogene. Geological Society of America Special Paper* 369: 395–412.
- JONES B. and MANNING D.A.C. 1994. Comparison of geochemical indices used for the interpretation of paleoredox conditions in ancient mudstones. *Chemical Geology* 111: 111–129.
- KAPLAN I.R. and RITTENBERG S.C. 1963. Microbiological fractionation of sulphur isotopes *Journal of General Microbiology* 34: 195–212.
- KOLTHOFF I.M. and SANDELL E.B. 1952. *Textbook of quantitative inorganic analysis*. MacMillan Company, New York: 759 pp.
- KRAJEWSKI K.P., VAN CAPPELEN P., TRICHET J., KUHN O., LUCAS J., MARTÍN-ALGARRA A., PRÉVÔT L., TEWARI V.C., GASPARD L., KNIGHT R.I. and LAMBOY M. 1994. Biological processes and apatite formation in sedimentary environments. *Eclogae Geologicae Helveticae* 87: 701–745.
- LI H. 1994. Some Late Cretaceous plants from King George Island, Antarctica. In: Y. Shen (ed.) *Stratigraphy and Palaeontology of Fildes Peninsula, King George Island, Antarctica. State Antarctic Committee, Monograph* 3: 85–96. Science Press, Beijing.

- LYONS T.W., WERNE J.P., HOLLANDER D.J. and MURRAY R.W. 2003. Contrasting sulfur geochemistry and Fe/Al and Mo/Al ratios across the last oxic-to-anoxic transition in the Cariaco Basin, Venezuela. *Chemical Geology* 195: 131–157.
- MACHEL H.G. 2001. Bacterial and thermochemical sulfate reduction in diagenetic settings – old and insights. *Sedimentary Geology* 140: 143–175.
- MANGALO M., MECKENSTOCK R.U., STICHLER W. and EINSIEDL F. 2007. Stable isotope fractionation during bacterial sulfate reduction is controlled by reoxidation of intermediates. *Geochimica et Cosmochimica Acta* 71: 4161–4171.
- MARINI L., GAMBARDELLA B., PRINCIPE C., ARIAS A., BROMBACH T. and HUNZICKER J.C. 2002. Characterization of magmatic sulfur in the Aegean island arc by means of the  $\delta^{34}\text{S}$  values of fumarolic  $\text{H}_2\text{S}$ , elemental S, and hydrothermal gypsum from Nisyros and Milos islands. *Earth and Planetary Science Letters* 200: 15–31.
- MARYNOWSKI L., RAKOCIŃSKI M. and ZATOŃ M. 2007. Middle Famennian (Late Devonian) interval with pyritized fauna from the Holy Cross Mountains (Poland): Organic geochemistry and pyrite framboid diameter study. *Geochemical Journal* 41: 187–200.
- MAZOT A., BERNARD A. and SUTAWIDJAJA I.S. 2007. Hydrothermal system of the Papandayan Volcano, West Java, Indonesia and its geochemistry evolution of thermal water after the November 2002 eruption. *Journal Geologi Indonesia* 2 (1): 15–29.
- MIDDELBURG J.J. 1991. Organic carbon, sulphur and iron in recent semi-euxinic sediments of Kau Bay, Indonesia. *Geochimica et Cosmochimica Acta* 55: 815–828.
- MORSE J.W., MILLERO F.J., CORNWELL J.C. and RICKARD D. 1987. The chemistry of the hydrogen sulfide and iron sulfide systems in natural waters. *Earth Sciences Review* 24: 1–42.
- OHFUJI H. and RICKARD D. 2005. Experimental syntheses of framboids – a review. *Earth Sciences Review* 71: 147–170.
- PANKHURST R.J. and SMELLIE J.L. 1983. K-Ar geochronology of the South Shetland Islands, Lesser Antarctica: apparent lateral migration of Jurassic to Quaternary island arc volcanism. *Earth and Planetary Science Letters* 66: 214–222.
- POOLE I., HUNT R.J. and CANTRILL D.J. 2001. A fossil wood flora from King George Island: ecological implications for an Antarctic Eocene vegetation. *Annals of Botany* 88: 33–54.
- RAISWELL R., BUCKLEY F., BERNER R.A., and ANDERSON T.F. 1988. Degree of pyritization of iron as a paleoenvironmental indicator of bottom-water oxygenation. *Journal of Sedimentary Research* 58: 812–819.
- RICKARD D., GRIMES S., BUTLER I., OLDROYD A. and DAVIES K.L. 2007. Botanical constraints on pyrite formation. *Chemical Geology* 236: 228–246.
- ROBERTS A.P. and TURNER G.M. 1993. Diagenetic formation of ferromagnetic iron sulphide minerals in rapidly deposited marine sediments. South Island, New Zealand. *Earth and Planetary Science Letters* 115: 257–273.
- SMELLIE J.L., PANKHURST R.J., THOMSON M.R.A. and DAVIES R.E.S. 1984. The geology of the South Shetland Islands. VI. Stratigraphy, geochemistry and evolution. *British Antarctic Survey, Scientific Reports* 87: 1–85.
- SWEENEY R.E. and KAPLAN I.R. 1973. Pyrite framboid formation: laboratory synthesis and marine sediments. *Economic Geology* 68: 618–634.
- TATUR A., KRAJEWSKI K.P., ANGIEL P., BYLINA P., DELURA K., MOZER A., NAWROCKI, J., PAŃCZYK M., PECSKAY Z. and ZIELIŃSKI G. 2009. Lithostratigraphy, dating and correlation of Cenozoic glacial and interglacial sequences on King George Island, West Antarctica. *First Antarctic Climate Evolution Symposium*, 7-11/09/2009, Granada, Spain. Abstract No. 3534.
- TAYLOR G.K. and MACQUAKER J.H.S. 2000. Early diagenetic pyrite morphology in a mudstone-dominated succession: the Lower Jurassic Cleveland Ironstone Formation, eastern England. *Sedimentary Geology* 131: 77–86.

- THODE H.G. 1991. Sulphur isotopes in nature and the environment: An overview. *In*: H.R. Krouse and V.A. Grinenko (eds) *Stable Isotopes: Natural and Anthropogenic Sulphur in the Environment*. SCOPE 43. J. Wiley & Sons, Chichester: 1–26.
- TORSSANDER P. 1992. Sulfur isotope ratios of leg 126 igneous rock. *Proceedings of the Ocean Drilling Program, Scientific Results* 126: 449–453.
- TUTTLE M.L., GOLDHABER M.B. and WILLIAMSON D.L. 1986. An analytical scheme for determining forms of sulphur in oil shales and associated rocks. *Talanta* 33: 953–961.
- UCHMAN A., GAŹDZICKI A. and BŁAŹEJOWSKI B. 2008. Caddisfly (Trichoptera) cases from the Oligocene lacustrine strata of King George Island, West Antarctica. *SCAR/IASC IPY, Open Science Conference. St. Petersburg, Russia, July 8th–11th 2008*. Abstract volume: 289–290.
- WANG Q. and MORSE J.W. 1996. Pyrite formation under conditions approximating those in anoxic sediments I. Pathways and morphology. *Marine Chemistry* 52: 99–121.
- WIGNALL P.B. and NEWTON R. 1998. Pyrite framboid diameter as a measure of oxygen deficiency in ancient mudrocks. *American Journal of Science* 298: 537–552.
- WIGNALL P.B., BOND D.P.G., KUWAHARA K., KAKUWA Y., NEWTON R.J. and POULTON S.W. 2010. An 80 million year oceanic redox history from Permian to Jurassic pelagic sediments of the Mino-Tamba terrane, SW Japan, and the origin of four mass extinctions. *Global and Planetary Change* 71: 109–123.
- WILKIN R.T. and BARNES H.L. 1997a. Formation processes of framboidal pyrite. *Geochimica et Cosmochimica Acta* 61: 323–338.
- WILKIN R.T. and BARNES H.L. 1997b. Pyrite formation in an anoxic estuarine basin. *American Journal of Science* 297: 620–650.
- WILKIN R.T., BARNES H.L. and BRANTLEY S.R. 1996. The size distribution of framboidal pyrite in modern sediments: An indicator of redox conditions. *Geochimica et Cosmochimica Acta* 60: 3897–3912.
- ZASTAWNIAK E. 1981. Tertiary leaf flora from the Point Hennequin Group of King George Island (South Shetland Islands, Antarctica). Preliminary report. *Studia Geologica Polonica* 72: 97–108.
- ZASTAWNIAK E. 1998. Plant vegetation in the Late Cretaceous and Tertiary of West Antarctica. *In*: A. Gaździcki A. and K. Jądzewski (eds) *Polar Ecosystems*. *Kosmos* 47 (4): 409–416 [in Polish, English summary].
- ZASTAWNIAK E., WRONA R., GAŹDZICKI A. and BIRKENMAJER K. 1985. Plant remains from the top part of the Point Hennequin Group (Upper Oligocene), King George Island (South Shetland Islands, Antarctica). *Studia Geologica Polonica* 81: 143–164.
- ZHOU Z. and LI H. 1994. Early Tertiary ferns from Fildes Peninsula, King George Island, Antarctica. *In*: Y. Shen (ed.) *Stratigraphy and Palaeontology of Fildes Peninsula, King George Island, Antarctica*. *State Antarctic Committee, Monograph* 3: 173–189. Science Press, Beijing.

Received 27 May 2010

Accepted 24 August 2010